Iron Isotope Fractionation During Magmatic Differentiation in Kilauea Iki Lava Lake

Fang-Zhen Teng,[1]*† Nicolas Dauphas,[1] Rosalind T. Helz[2]

Magmatic differentiation helps produce the chemical and petrographic diversity of terrestrial rocks. The extent to which magmatic differentiation fractionates nonradiogenic isotopes is uncertain for some elements. We report analyses of iron isotopes in basalts from Kilauea Iki lava lake, Hawaii. The iron isotopic compositions ($^{56}Fe/^{54}Fe$) of late-stage melt veins are 0.2 per mil (‰) greater than values for olivine cumulates. Olivine phenocrysts are up to 1.2‰ lighter than those of whole rocks. These results demonstrate that iron isotopes fractionate during magmatic differentiation at both whole-rock and crystal scales. This characteristic of iron relative to the characteristics of magnesium and lithium, for which no fractionation has been found, may be related to its complex redox chemistry in magmatic systems and makes iron a potential tool for studying planetary differentiation.

Studies of isotopic variations in terrestrial and extraterrestrial rocks can be used to identify the processes that govern planetary differentiation. For example, Fe isotopic compositions of lunar and terrestrial basalts are slightly heavier than those of chondrites, Mars, and Vesta; this has been ascribed to evaporation-induced kinetic fractionation of Fe isotopes during the giant impact that formed the Moon (*1*). This interpretation assumes that the Fe isotopic composition of basalts is representative of the source composition (i.e., mantle), which is supported by isotopic studies of other elements like Li and Mg (*2*, *3*). Although studies of mantle peridotites have shown measurable Fe isotope fractionation during mantle melting (*4*, *5*), the effect of fractional crystallization on Fe isotopes remains uncertain (*6*–*10*). Many processes—such as partial melting, magma mixing, assimilation of country rocks, fractional crystallization, and late-stage fluid exsolution—can affect Fe isotope systematics of the magma before it reaches the surface. Isotopic variations may result from different processes, and it is difficult to identify the contributions of specific processes to the observed isotopic signatures.

To isolate and evaluate the influence of fractional crystallization, we worked on a set of well-characterized samples from Kilauea Iki lava lake, Hawaii. Kilauea Iki lava lake formed during the 1959 summit eruption of Kilauea volcano by filling a previously existing crater (Fig. 1). After the formation of a stable crust at the end of the eruption, the lava lake cooled and crystallized as a small, self-roofed, closed magma chamber surrounded on all sides by partially molten regions and extending outward to fully solidified rocks (*11*, *12*). It was drilled repeatedly from 1960 to 1988, resulting in almost 1200 m of drill cores. We analyzed two 1959 eruption samples (IKI-22 and IKI-58) and a variety of drill core samples, ranging from olivine-rich cumulates to andesitic segregation veins, to cover the whole spectrum of chemical compositions, mineralogies, and crystallization temperatures (*12*).

The $\delta^{56}Fe$ values $\{\delta^{56}Fe = [(^{56}Fe/^{54}Fe)_{sample}/(^{56}Fe/^{54}Fe)_{IRMM\text{-}014} - 1] \times 1000\}$ of all the whole-rock samples vary inversely with MgO and total FeO contents (Fe_2O_3 and FeO calculated as FeO_{total}) and directly with $Fe^{3+}/\sum Fe$ ratios ($\sum Fe = Fe^{3+} + Fe^{2+}$) (Fig. 2). Olivine cumulates have high MgO contents [up to 26.87 weight percent (wt %)] and low $\delta^{56}Fe$ values (down to –0.03‰), whereas late-stage veins have low MgO contents (down to 2.37 wt %) and high $\delta^{56}Fe$ values (up to +0.22‰) (table S1). The Fe isotopic compositions of 42 olivine grains, separated from two drill core samples, display a larger Fe isotopic variation, ranging from –1.10 to +0.09‰ (Fig. 3). The variations are irrespective of the olivine crystal weight (table S2). The average $\delta^{56}Fe$ of these olivine grains is -0.22 ± 0.08‰ [95% confidence interval (CI)], which is significantly lower than that of the two whole rocks (i.e., +0.11 and +0.12‰).

The large chemical variations in Kilauea Iki lavas mainly resulted from posteruptive redistribution of olivine phenocrysts, followed by crystallization of pyroxene, plagioclase, and Fe-Ti oxide phases as the lava lake cooled (*11*). Both equilibrium (*7*, *8*, *13*, *14*) and kinetic (*15*–*17*) Fe isotope fractionation between minerals and melts could happen during fractional crystallization and produce the observed Fe isotopic variations in the lava lake.

During the process of isotope fractionation, Fe isotopic variations in the samples with MgO < 11 wt %, which mainly result from fractional crystal-

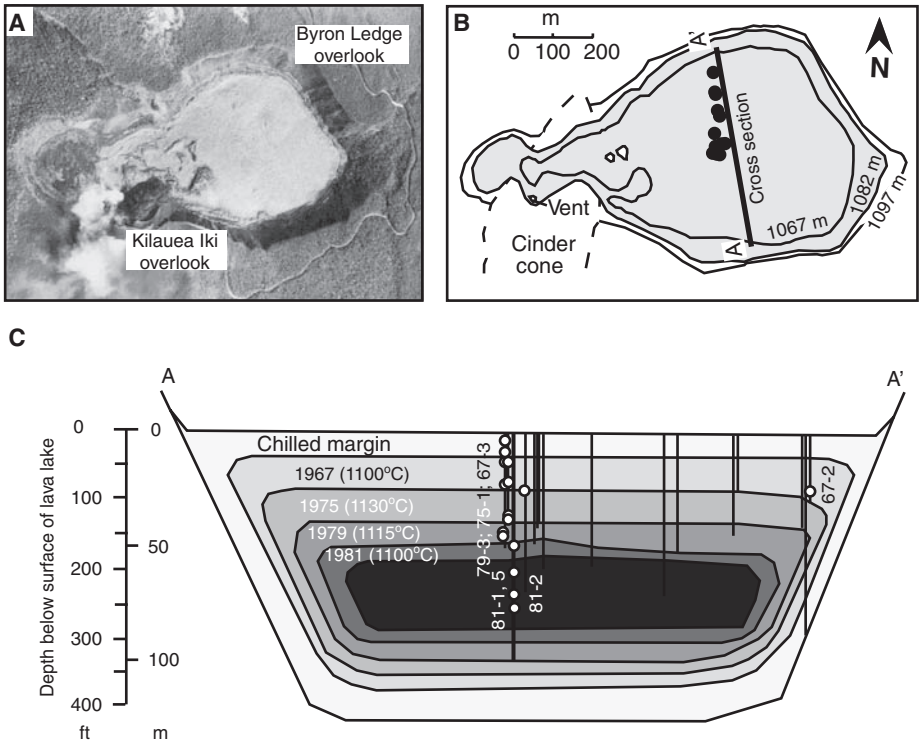

Fig. 1. (**A**) Aerial photograph (*26*) taken immediately after the 1959 eruption of Kilauea volcano, showing the surface of the newly formed Kilauea Iki lava lake. (**B**) Plan view of the posteruptive surface of Kilauea Iki lava lake. The black circles indicate locations of holes drilled between 1967 and 1988. Numbers on contour lines are elevations above sea level. (**C**) Cross section of Kilauea Iki lava lake with a vertical exaggeration of 2:1. The vertical lines show locations of drill holes or closely spaced clusters of drill holes, projected onto this cross section. The concentric zones show the limit of drillable crust and temperatures at different years. Only the drill holes that are labeled indicate where samples (white circles) came from in this study.

[1]Origins Laboratory, Department of the Geophysical Sciences and Enrico Fermi Institute, University of Chicago, 5734 South Ellis Avenue, Chicago, IL 60637, USA. [2]United States Geological Survey, Reston, VA 20192, USA.

*Present address: Isotope Laboratory, Department of Geosciences and Arkansas Center for Space and Planetary Sciences, University of Arkansas, 113 Ozark Hall, Fayetteville, AR 72701, USA.
†To whom correspondence should be addressed. E-mail: fteng@uark.edu

lization (*11*), can be modeled by Rayleigh fractionation with average crystal-melt fractionation factors ($\Delta\delta^{56}$Fe) of ~ –0.1 to –0.3‰ (Fig. 4). For a given δ^{56}Fe of the original melt of ~ +0.1‰, the predicted δ^{56}Fe of the minerals are ~ 0 to –0.2‰. These values, in turn, are used to model the compositions of samples with MgO > 11 wt %, which are composed of melt + olivine phenocrysts (*11*), by mixing the assumed composition of the most Mg-rich melt (δ^{56}Fe = +0.11‰) with that of the predicted olivine crystals (δ^{56}Fe = 0 to –0.2‰) (Fig. 4) (*12*).

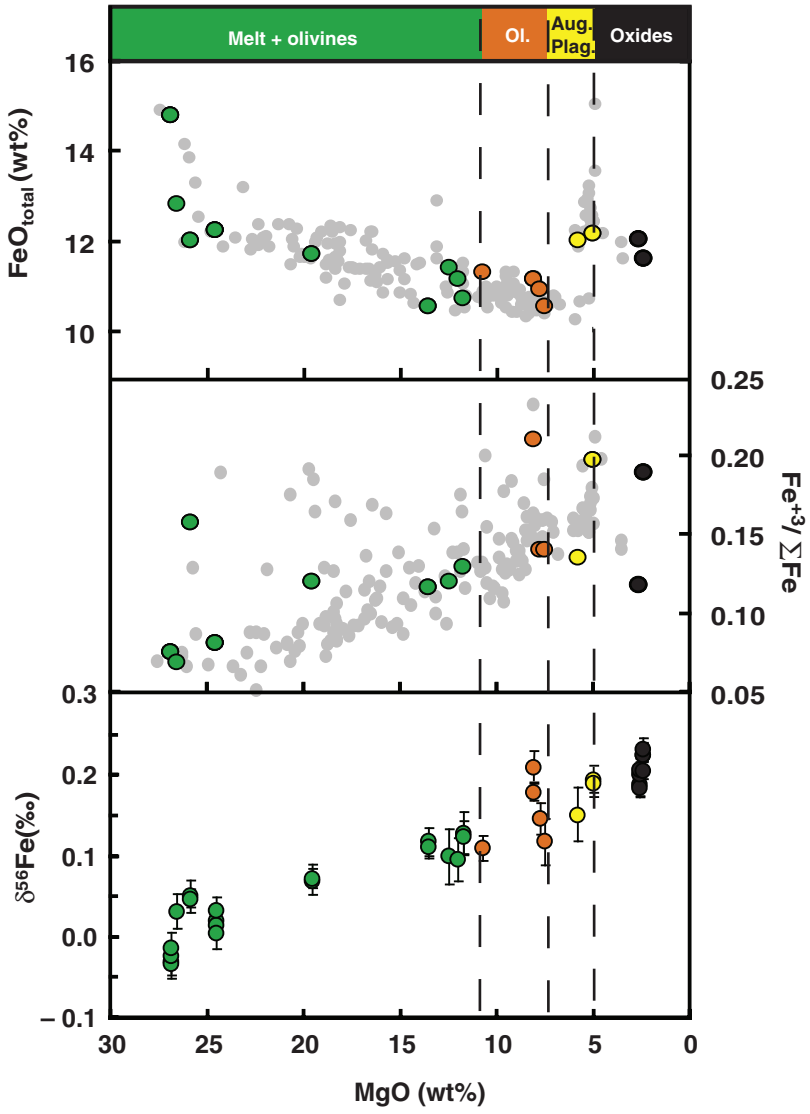

Fig. 2. Variations of FeO_{total}, $Fe^{3+}/\sum Fe$ ratios, and δ^{56}Fe values as a function of MgO contents in whole-rock samples. Samples with MgO > 11 wt % are melt + olivine phenocrysts, whereas those with MgO < 11 wt % reflect fractional crystallization of olivine (Ol.), followed by augite (Aug.), plagioclase (Plag.), and Fe-Ti oxides (*11*). Gray circles represent all samples from Kilauea Iki lava lake (*27*). Error bars indicate 95% CI of the mean. Data from table S1.

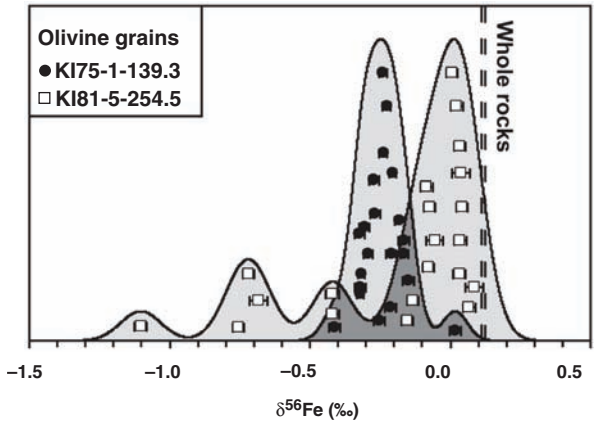

Fig. 3. Iron isotopic compositions of olivine grains from Kilauea Iki lava lake. The curves are kernel density estimates with automatic bandwidth selection and have the same surface area. The dashed lines are the δ^{56}Fe values (+0.11 and +0.12‰) of those two whole rocks. Error bars indicate 95% CI of the mean. Data from tables S1 and S2.

Although no experimentally calibrated equilibrium fractionation factor for olivine melt is currently available, the fractionation factors that fit the whole-rock data generally agree with theoretical calculations (*13*, *14*), experimental studies on fractionation of pyrrhotite and silicate melt (*7*), and fractionation of olivine and magnetite (*8*). These results are also consistent with the range of Fe isotope fractionation during mantle melting (*4*, *5*). However, olivine phenocrysts from the lava lake are highly varied and have δ^{56}Fe values well beyond the range defined by the equilibrium isotope fractionation model (Fig. 4). Segregation veins and some diapirs are known to have formed as the lake crystallized (*18*). The diapirs transferred olivines from the cumulate zone into differentiated liquid (*18*). These processes affected the whole column of "mush" and could have magnified the equilibrium fractionation of Fe isotopes in the olivine in a way that is analogous to isotope fractionation during chromatography (*19*). Different olivine grains in the lake might have experienced these processes to different extents and hence display different degrees of isotope fractionation.

Alternatively, significant high-temperature kinetic fractionation of Mg and Fe isotopes has been documented during thermal diffusion in silicate melts (*16*, *17*, *20*) and chemical diffusion between molten basalt and rhyolite (*16*, *20*). Substantial thermal gradients were observed in the lava lake throughout its crystallization history; the cumulate zone was hotter than the surrounding partially molten zone, and temperature gradients within the partially molten zone reached up to 65°C/m vertically (*21*). Because the hot end was always enriched with light isotopes during thermal diffusion experiments (*16*, *17*, *20*), these thermal gradients may have driven Fe diffusion and Fe isotope fractionation in both whole rocks and olivines, enriching the olivine cumulates in the light isotopes of Fe (and the light isotopes of Mg).

In addition to thermal diffusion, kinetic isotope fractionation can also happen by chemical diffusion. This could have happened during diffusion-limited crystal growth, where light isotopes can be supplied to the growing crystal at a faster rate than heavy isotopes resulting from differences in diffusivities (*15*, *22*). Fractionation could also have taken place during chemical re-equilibration of olivines in the course of cooling and crystallization of the lava lake. The olivines from samples quenched at lower temperature are more Fe-rich and show more scatter in composition than those from samples quenched at higher temperature (fig. S1) (*12*), which reflects re-equilibration of the olivines with evolving residual melts (*23*). Diffusion of Fe from the melt into the interior of the olivine phenocrysts should be associated with kinetic isotope fractionation, thereby enriching the partially equilibrated

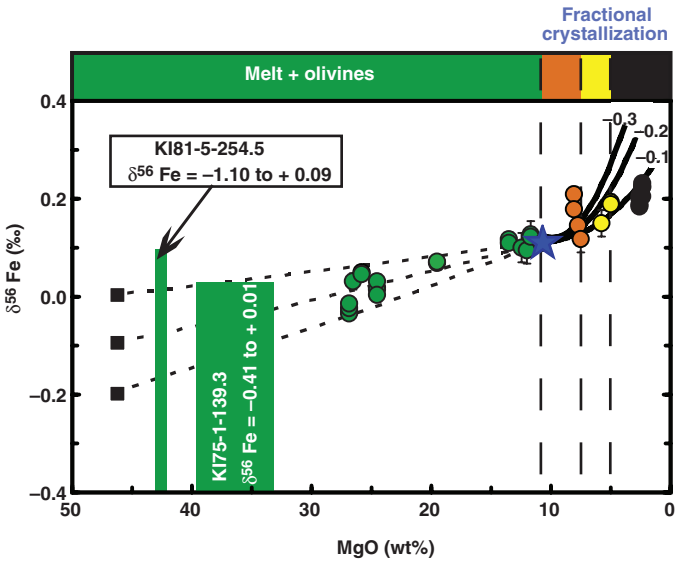

Fig. 4. Modeling of Fe isotopic variations during magmatic differentiation in Kilauea Iki lava lake (*12*). Solid lines represent calculated Fe isotopic compositions of residual melts during fractional crystallization by assuming a Rayleigh distillation process with average crystal-melt fractionation factors ($\Delta\delta^{56}Fe_{crystal\text{-}melt} = \delta^{56}Fe_{crystal} - \delta^{56}Fe_{melt}$) of –0.1, –0.2, and –0.3‰. Dashed horizontal lines represent calculated mixing lines between the most magnesian melt from the 1959 eruption (*23*) and the most magnesian olivines [(MgO = 46.6 ± 1 wt % and δ^{56}Fe = 0, –0.1, and –0.2‰ (black squares)]. The blue star represents the most magnesian melt (MgO = 10.7 wt %; assumed δ^{56}Fe = 0.11‰). The green bars represent the ranges of measured δ^{56}Fe and estimated MgO in olivine grains from two drill core samples (MgO = 33.6 to 39.8 wt % and 41.9 to 42.7 wt %; table S3). Sample crystallization sequences are the same as those in Fig. 2. Error bars indicate 95% CI of the mean.

olivines in the light isotopes of Fe (and the heavy isotopes of Mg) (*16*, *20*).

The extent of equilibrium isotope fractionation is mainly controlled by the relative mass difference between the isotopes, and more fractionation happens in isotopes with a larger relative mass difference (*14*, *24*). If the Fe isotopic variation in the lava lake was produced by equilibrium isotope fractionation, Mg isotopes should show more significant fractionation than Fe isotopes because of their larger relative mass difference. Furthermore, kinetic isotope fractionation driven by thermal and chemical diffusion should also result in larger fractionation in Mg isotopes as compared with that in Fe isotopes (*16*, *17*, *20*). The absence of Mg isotope fractionation in Kilauea Iki lavas may result from the low-precision isotopic analysis of Mg relative to Fe (e.g., 0.1 versus 0.04), which prevents the detection of Mg isotopic variation. More likely, the presence of Fe isotope fractionation and the absence of Mg isotope fractionation may reflect the influence of Fe oxidation states on kinetic or equilibrium isotope fractionation (as compared with those of Mg, two oxidation states of Fe exist in terrestrial magmatic systems) (*5*, *25*).

Our study suggests that, unlike Li and Mg isotopes (*2*, *3*), Fe isotopes fractionate during basaltic differentiation at both whole-rock and crystal scales. Mineral compositions should therefore be used to help interpret whole-rock basalt Fe isotopic data. The elevated δ^{56}Fe of crustal igneous rocks, which is more evolved than that in basalts, could be explained by fractional crystallization (*10*).

References and Notes

1. F. Poitrasson, A. N. Halliday, D. C. Lee, S. Levasseur, N. Teutsch, *Earth Planet. Sci. Lett.* **223**, 253 (2004).
2. F.-Z. Teng, M. Wadhwa, R. T. Helz, *Earth Planet. Sci. Lett.* **261**, 84 (2007).
3. P. B. Tomascak, F. Tera, R. T. Helz, R. J. Walker, *Geochim. Cosmochim. Acta* **63**, 907 (1999).
4. S. Weyer, D. A. Ionov, *Earth Planet. Sci. Lett.* **259**, 119 (2007).
5. H. M. Williams *et al.*, *Earth Planet. Sci. Lett.* **235**, 435 (2005).
6. B. L. Beard *et al.*, *Chem. Geol.* **195**, 87 (2003).
7. J. A. Schuessler, R. Schoenberg, H. Behrens, F. von Blanckenburg, *Geochim. Cosmochim. Acta* **71**, 417 (2007).
8. A. Shahar, C. E. Manning, E. D. Young, *Earth Planet. Sci. Lett.* **268**, 330 (2008).
9. R. Schoenberg, F. von Blanckenburg, *Earth Planet. Sci. Lett.* **252**, 342 (2006).
10. F. Poitrasson, R. Freydier, *Chem. Geol.* **222**, 132 (2005).
11. R. T. Helz, in *Magmatic Processes: Physicochemical Principles*, B. O. Mysen, Ed. (Geochemical Society, University Park, PA, 1987), vol. 1, pp. 241–258.
12. Materials, methods, data, and modeling details are available as supporting material on *Science* Online.
13. V. B. Polyakov, R. N. Clayton, J. Horita, S. D. Mineev, *Geochim. Cosmochim. Acta* **71**, 3833 (2007).
14. E. A. Schauble, in *Geochemistry of Non-Traditional Stable Isotopes*, C. M. Johnson, B. L. Beard, F. Albarede, Eds. (Mineralogical Society of America, Washington, DC, 2004), vol. 55, pp. 65–111.
15. N. Dauphas, O. Rouxel, *Mass Spectrom. Rev.* **25**, 515 (2006).
16. F. M. Richter, *Geochim. Cosmochim. Acta* **71**, A839 (2007).
17. F. Huang, C. C. Lundstrom, A. J. Ianno, *Geochim. Cosmochim. Acta* **71**, A422 (2007).
18. R. T. Helz, H. Kirschenbaum, J. W. Marinenko, *Geol. Soc. Am. Bull.* **101**, 578 (1989).
19. A. D. Anbar, J. E. Roe, J. Barling, K. H. Nealson, *Science* **288**, 126 (2000).
20. F. M. Richter, E. B. Watson, R. A. Mendybaev, F.-Z. Teng, P. E. Janney, *Geochim. Cosmochim. Acta* **72**, 206 (2008).
21. R. T. Helz, C. R. Thornber, *Bull. Volcanol.* **49**, 651 (1987).
22. A. Jambon, *Geochim. Cosmochim. Acta* **44**, 1373 (1980).
23. R. T. Helz, *U.S. Geol. Surv. Prof. Pap.* **1350**, 691 (1987).
24. H. C. Urey, *J. Chem. Soc. (London)* **1947**, 562 (1947).
25. H. M. Williams *et al.*, *Science* **304**, 1656 (2004).
26. D. H. Richter, J. P. Eaton, K. J. Murata, W. U. Ault, H. L. Krivoy, *U.S. Geol. Surv. Prof. Pap.* **537-E**, 1 (1970).
27. R. T. Helz, H. Kirschenbaum, J. W. Marinenko, R. Qian, *U.S. Geol. Surv. Open-File Rep.* **94-684**, 1 (1994).

28. Discussions with S. Huang, A. T. Anderson Jr., F. M. Richter, M. Wadhwa, P. B. Tomascak, R. J. Walker, and A. Pourmand are appreciated. We thank three anonymous reviewers for constructive comments. This work was supported by a Packard fellowship, the France Chicago Center, and NASA through grant NNG06GG75G to N.D.

Supporting Online Material

www.sciencemag.org/cgi/content/full/320/5883/1620/DC1
SOM Text S1 to S5
Fig. S1
Tables S1 to S4
References

29 February 2008; accepted 12 May 2008
10.1126/science.1157166

Natural Variability of Greenland Climate, Vegetation, and Ice Volume During the Past Million Years

Anne de Vernal* and Claude Hillaire-Marcel

The response of the Greenland ice sheet to global warming is a source of concern notably because of its potential contribution to changes in the sea level. We demonstrated the natural vulnerability of the ice sheet by using pollen records from marine sediment off southwest Greenland that indicate important changes of the vegetation in Greenland over the past million years. The vegetation that developed over southern Greenland during the last interglacial period is consistent with model experiments, suggesting a reduced volume of the Greenland ice sheet. Abundant spruce pollen indicates that boreal coniferous forest developed some 400,000 years ago during the "warm" interval of marine isotope stage 11, providing a time frame for the development and decline of boreal ecosystems over a nearly ice-free Greenland.

The potential for sea-level rise, caused by melting of the Greenland ice-sheet as surface air temperature increases, is considerable (*1*). Although there is evidence that the velocity of ice streams flowing into the ocean and the rate of thinning of the ice have increased recently (*2*, *3*), large uncertainties remain about the long-term stability of the ice sheet. The climate

www.sciencemag.org/cgi/content/full/320/5883/1620/DC1

Supporting Online Material for

Iron Isotope Fractionation During Magmatic Differentiation in Kilauea Iki Lava Lake

Fang-Zhen Teng,* Nicolas Dauphas, Rosalind T. Helz

*To whom correspondence should be addressed. E-mail: fteng@uark.edu

Published 20 June 2008, *Science* **320**, 1620 (2008)

DOI: 10.1126/science.1157166

This PDF file includes:

Supporting Online Material

SOM1. Whole-rock samples

The Kilauea volcano is located on the southeastern side of the island of Hawaii. Kilauea Iki lava lake lies near the summit of Kilauea volcano, east of its main caldera, and was formed during the 1959 summit eruption of Kilauea volcano (*S1, S2*). Kilauea Iki lava lake was drilled over the period 1960-1988. The quenched drill core samples are instantaneous records of the processes that were active during the cooling of the lava lake. Therefore, the Kilauea Iki lava lake provides an ideal field laboratory for studying magmatic differentiation (*S3*).

The original 1959 Kilauea Iki lava consists of picritic tholeiite and is composed of glass + olivine and chromite crystals, with an average MgO content of 15.43 wt.% (*S2*). Glass compositions in eruption samples range from 6.5 to 10.0 wt.% MgO (*S4*). The olivine phenocrysts include several distinct subpopulations, derived from different levels of Kilauea's plumbing (*S4*). Internal differentiation of the lava lake has produced a variety of rock types from olivine-rich cumulates, through olivine tholeiites, to ferrodiabase and more silicic veins, and large chemical variations with MgO content ranging from 2.37 to 26.87 wt.% (*S4*). Rocks with MgO contents >7.0 wt.% contain olivine phenocrysts in a fine-grained groundmass of glass, clinopyroxene, plagioclase, and opaque minerals in varying amounts (*S4, S5*) and have been affected predominantly by settling of olivine crystals while highly differentiated rocks with MgO contents <7.0 wt.% have been produced by segregation of liquid from within coherent, crystal-rich mushes (*S3,S4*). The quenching temperature of these samples, as estimated by the MgO content of glass (*S6*) or from thermocouple data, ranges from greater than 1216 ^{o}C down to 1055 ^{o}C (*S6*).

Eighteen well-studied samples covering the whole compositional and mineralogical spectrum of the Kilauea Iki lava, including two original eruption samples (Iki-22 and Iki-58) and 16 drill core samples from the interior of the lake, were analyzed to ascertain whether there is any Fe isotopic variation during basaltic differentiation. Nine

of the drill core samples in this study were entirely crystalline when drilled while seven of them (samples KI81-1-239.9, KI81-1-210, KI75-1-139.3, KI67-3-81, KI79-3-158.0, KI67-2-85.7, KI81-5-254.5) consisted of a liquid-crystal "mush" in which the interstitial melt was quenched by the drilling process.

SOM2. Olivine grains

Olivine phenocrysts in the eruption samples preserve a significant amount of internal disequilibrium and are moderately zoned (<3% Fo) with normally and reversely zoned crystals in about equal amounts (*S7*). The presence of variable zoning patterns within samples have been attributed to magma mixing (*S2, S7*). On average, the Fo contents of olivines in the eruption samples are relatively homogenous ($Fo_{86\pm1}$). In contrast, olivines collected by drilling cores from the Kilauea Iki lava lake are all normally zoned, may vary by 5% Fo or more, and have re-equilibrated with the melt during slow cooling (*S7*). The Fo contents of olivines from the lave lake reflect the re-equilibration process and vary significantly with quenching temperatures. Cores of coarse olivines in samples quenched from high temperatures have higher Fo contents than those quenched from lower temperatures (Fig. S1 and Table S3).

Olivine grains have been picked up from two drill core samples. One sample was quenched from relatively high temperature (KI81-5-254.5, 1134 ^{o}C) and the other one was quenched from relatively low temperature (KI75-1-139.3, 1070 ^{o}C) (Table S2). No Fo data are available for these olivine grains but Fo contents in other olivines from the same sample (KI75-1-139.3) have been analyzed (Table S3) and vary from 67 to 76. The Fo contents of olivines from sample KI81-5-254.5 are estimated from the trend in Fig. S1: olivines with quench temperatures of 1135 ^{o}C in the lava lake have a limited range in Fo contents from 79.7 to 81.7. This range is used to represent that of olivines from sample KI81-5-254.5 with a quench temperature of 1134 ^{o}C.

In addition to olivines, sample KI75-1-139.3 contains melt, augite, pigeonite, plagioclase and ilmenite, and sample KI81-5-254.5 contains melt, augite and plagioclase. These additional mineral phases are too small to separate for isotopic analysis.

SOM3. Analytical Method

The whole-rock powders studied here have been used in previous studies *(S3, S4, S8, S9, S10)*. The olivine grains were prepared as follows: Almost pure (>98%) olivine grains were handpicked under a binocular microscope, cleaned with Milli-Q water for 3×10 minutes in an ultrasonic bath, and dried down under a heat lamp before dissolution. Both whole-rock powders and olivine separates were dissolved in a combination of HF-$HClO_4$-HNO_3. Iron was purified on anion exchange resin (AG1-X8 200-400 mesh) in HCl medium by the established procedure of Dauphas et al. (*S11,S12*). Its isotopic composition was analyzed by using a Neptune high-resolution MC-ICPMS installed at the Origins Laboratory, The University of Chicago. The long-term precision, based on replicate analyses of granites, basalts, and chondrites, is ≤0.04‰ (95 % confidence interval).

The accuracy was assessed in several ways. First, Fe isotopic compositions of well-characterized international standards analyzed in our lab agree well with published values (Table S4). Second, IRMM-014 was added to the eluted matrix fractions of several well-characterized samples in quantities that matched the Fe contents of the original samples and these mixtures were then processed through columns and analyzed as unknowns. The results show that these mixtures are isotopically indistinguishable from unprocessed IRMM-014 within 0.03 ‰. Finally, eluted Fe and matrix fractions of four end-member basalt samples were collected and interchanged (KI81-2-88.6 vs. KI81-1-169.9; KI67-2-85.7 vs. KI81-1-210). The results show that these mixtures have Fe isotopic compositions identical to their original samples. These tests demonstrate that we are able to measure both accurately and precisely the Fe isotopic compositions of natural samples at the level of precision reported in Table S4.

SOM4. Rayleigh distillation model in Fig. 4

The equation that governs isotopic fractionation in a Rayleigh distillation process is $(\delta^{56}Fe)_{melt} = [(\delta^{56}Fe)_{initial\ melt} +1000]f^{(\alpha-1)} -1000$, where the fractionation factor is $\alpha = (^{56}Fe/^{54}Fe)_{crystal} / (^{56}Fe/^{54}Fe)_{melt}$, the fraction of Fe remaining in the melt is $f = F \times C_{m,FeO}/C_{i,FeO}$, (i and m subscripts refer to initial and melt, respectively). F is the

fraction of melt remaining and is calculated from the following equation based on the K_2O concentrations of the samples (the concentration of an incompatible element is easily related to the fraction of crystals that have been removed from the system): $C_{m,K2O} = C_{i,K2O} \times F^{(D-1)}$, where $D = K_{crystal} / K_{melt} = 0.04$ (*S13*). $C_{m,FeO}$ is the FeO concentration in the remaining melt and $C_{i,FeO}$ is the Fe concentration in the initial melt.

Since samples with MgO <11 wt% reflect fractional crystallization of olivine , augite, plagioclase and Fe-Ti oxides (*S4*) and no sample with 11 wt% MgO has been analyzed, the sample KI67-3-39 (MgO = 10.73 wt%, total FeO = 11.32 wt%, K_2O = 0.54 wt% and $\delta^{56}Fe$ = 0.11 ‰) is taken to represent the composition of the initial melt in the calculation ($C_{i,FeO}$ = 11.32 wt%). The FeO concentration in the remaining melt, $C_{m,FeO}$, is represented by the FeO concentrations measured in the samples.

SOM5. Mixing model in Fig. 4

The equation that governs mixing of 2 end-members is $\delta^{56}Fe = (\delta^{56}Fe)_1 \times f_1 + (\delta^{56}Fe)_0 \times (1-f_1)$, where f_1 is the fraction of Fe from the end member 1. Dashed lines represent calculated mixing lines between the most magnesian melt and olivines. Olivines from the eruption samples have the highest Fo contents (85-88% Fo (*S7*), corresponding MgO contents of 45.5- 47.7 wt%) and this chemical composition has been used as an end member in the mixing calculation.

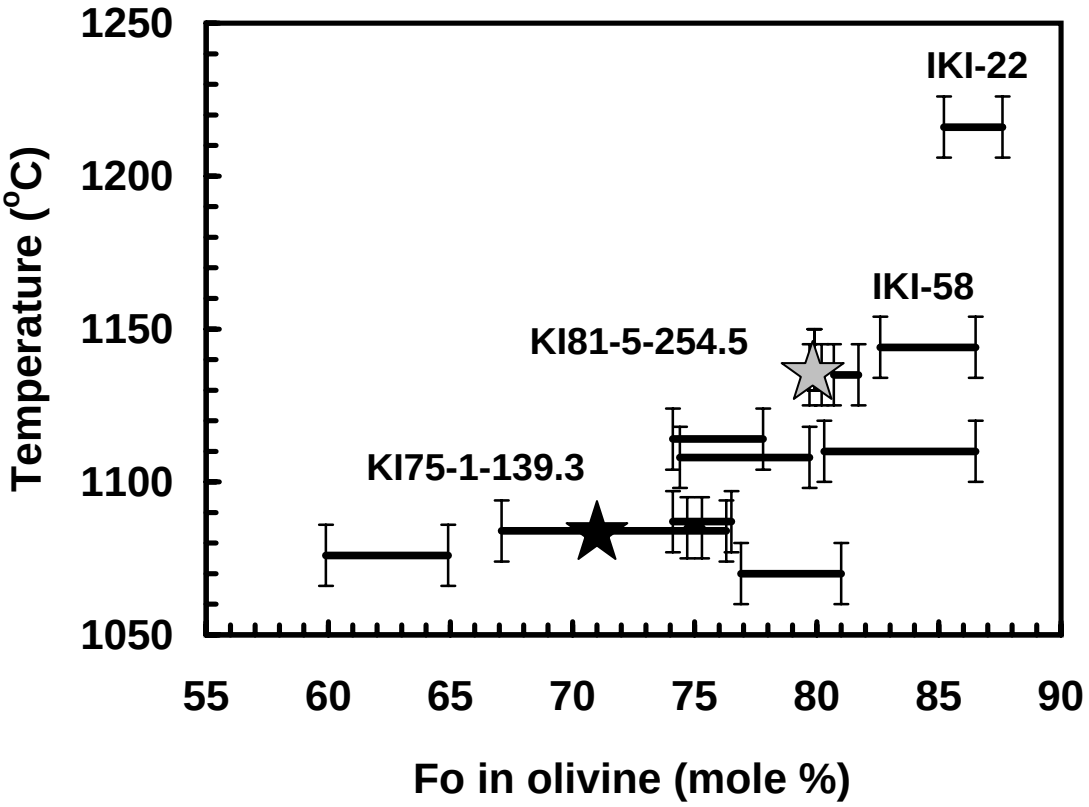

Figure S1.Variations of quench temperatures of whole rocks vs. the range of Fo content in olivine grains. Olivines become progressively more Fe-rich as the temperature decreases and show more scatter in the lower-temperature samples, reflecting partial reequilibration of olivines with evolving residual melts. Data for the maximum and minimum Fo contents in olivine grains from Table S4. The Fo content of sample KI81-5-254.5 is estimated based on the quench temperature of 1134 ^{o}C. See SOM1 and SOM2 for details.

Table S1 Iron isotopic data of whole-rock samples from Kilauea Iki lava lake, Hawaii

Sample	MgO (wt.%)	SiO_2 (wt.%)	K_2O (wt.%)	FeO_{total} (wt.%)	$Fe^{3+}/\sum Fe$	T (^oC)	$\delta^{26}Mg$	$\delta^{56}Fe$	95 % c.i.	$\delta^{57}Fe$	95 % c.i.
KI81-1-169.9	26.87	43.71	0.25	14.80	0.08		-0.34	-0.031	0.027	-0.039	0.038
Cu doping								-0.034	0.024	-0.041	0.047
Rep. Cu doping								-0.024	0.027	-0.044	0.041
Matrix doping								-0.014	0.026	-0.009	0.070
KI81-1-239.9	26.55	44.21	0.20	12.81	0.07	1140		0.031	0.029	0.039	0.028
KI67-3-6.8	25.83	44.63	0.30	12.02	0.16		-0.32	0.050	0.026	0.063	0.045
Cu doping								0.046	0.024	0.084	0.047
KI81-1-210	24.53	44.87	0.21	12.23	0.08	1135	-0.31	0.019	0.027	0.019	0.038
Cu doping								0.014	0.024	0.029	0.047
Rep. Cu doping								0.031	0.027	0.038	0.041
Matrix doping								0.004	0.026	0.001	0.070
IKI-22	19.52	46.68	0.35	11.71	0.12	1216	-0.37	0.069	0.027	0.098	0.038
Cu doping								0.072	0.024	0.108	0.047
KI79-3-150.4	13.51	48.44	0.44	10.54	0.12		-0.41	0.117	0.027	0.176	0.038
Cu doping								0.110	0.022	0.169	0.047
KI75-1-38.9	12.46			11.40	0.12		-0.40	0.100	0.042	0.150	0.064
KI67-3-27.5*	12.01	48.61	0.49	11.16	0.27			0.095	0.039	0.126	0.060
KI75-1-139.3	11.70	48.77	0.52	10.73	0.13	1084		0.127	0.039	0.184	0.060
replicate								0.123	0.032	0.182	0.044
KI67-3-39*	10.73	48.90	0.54	11.32	0.33		-0.39	0.109	0.038	0.176	0.041
IKI-58	8.08	49.91	0.55	11.16	0.21	1144	-0.42	0.209	0.038	0.305	0.041
Cu doping								0.178	0.022	0.264	0.047
KI67-3-81	7.73	49.75	0.63	10.94	0.14	1055	-0.35	0.146	0.029	0.184	0.038
KI75-1-121.5	7.50	50.00	0.64	10.55	0.14		-0.40	0.118	0.039	0.179	0.060
KI75-1-75.2	5.77	50.13	0.79	12.02	0.13		-0.29	0.150	0.039	0.230	0.060
KI79-3-158.0	5.00			12.17	0.20	990		0.193	0.028	0.289	0.041
Cu doping								0.189	0.022	0.293	0.047
KI67-2-85.7	2.60	56.21	1.99	12.03	0.12	1060	-0.35	0.188	0.028	0.288	0.041
Cu doping								0.184	0.022	0.271	0.047
Rep. Cu doping								0.201	0.027	0.289	0.047
Matrix doping								0.206	0.026	0.321	0.070
KI81-2-88.6	2.37	57.07	1.90	11.61	0.19		-0.41	0.224	0.028	0.337	0.041
Cu doping								0.205	0.022	0.310	0.047
Rep. Cu doping								0.224	0.027	0.340	0.041
Matrix doping								0.232	0.026	0.398	0.070
KI81-5-254.5						1134		0.111	0.038	0.141	0.044

The sample number is given first by the drill core number, followed by the depth of the sample in feet: e.g., sample KI81-1-169.9 comes from core KI81-1, 169.9 feet below the surface of the lava lake. Major elemental data from Helz et al. (*S8*) with uncertainties of less than 1% (*S14*); $Fe^{3+}/\sum Fe$ is mole ratio of Fe^{3+} in Fe_2O_3 and total Fe (Fe^{3+} in Fe_2O_3 + Fe^{2+} in FeO), and quench temperatures are estimated for samples consisting of a liquid-crystal "mush" by the MgO geothermometry (*S6*). $\delta^{26}Mg$ data from Teng et al. (*S9*), with an external precision of ±0.1‰. $\delta^{x}Fe = [(^{x}Fe/^{54}Fe)_{sample}/ (^{x}Fe/^{54}Fe)_{standard} -1] \times 1000$, where standard = IRMM-014 and x = 56 or 57); 95 % c.i. stands for 95 % confidence interval of the mean (for 9 replicate analyses of the same solution) and it integrates the long-term reproducibility based on replicate analyses of BHVO-1 standard (*S12*). Cu doping: solutions analyzed by Cu doping method besides sample-standard bracketing method (*S15*); replicate: repeat column chemistry from the same stock sample solution and analyzed by sample-standard bracketing method; Rep. Cu doping; repeat column chemistry from the same stock sample solution analyzed by Cu doping method; Matrix doping: eluted Fe and matrix fractions of four end-member basalt samples were collected and interchanged (KI81-2-88.6 vs. KI81-1-169.9; KI67-2-85.7 vs. KI81-1-210). The mixing solutions were then processed through columns and analyzed as unknowns. Samples marked with "*" are subsolidus samples that have been oxidized by exposure to air in the upper parts of the lake, and therefore their $Fe^{3+}/\sum Fe$ ratios do not reflect initial values.

Table S2 Iron isotopic compositions of olivine grains from Kilauea Iki lava lake, Hawaii

KI81-5-254.5						KI75-1-139.3					
Sample	wt. (mg)	δ^{56}Fe	95 % c.i.	δ^{57}Fe	95 % c.i.	Sample	wt. (mg)	δ^{56}Fe	95 % c.i.	δ^{57}Fe	95 % c.i.
Ol-1	0.56	-0.755	0.032	-1.112	0.044	Ol-1	0.75	-0.253	0.032	-0.406	0.044
Ol-2	0.72	-0.721	0.032	-1.078	0.044	Ol-2	0.47	-0.149	0.032	-0.284	0.044
Ol-3	0.24	+0.032	0.032	+0.007	0.044	Ol-3	0.69	-0.412	0.032	-0.634	0.044
Ol-4	0.37	-0.073	0.032	-0.110	0.044	Ol-4	0.79	+0.017	0.032	-0.137	0.044
Ol-5	0.71	+0.005	0.032	+0.010	0.044	Ol-5	0.49	-0.212	0.032	-0.341	0.044
Ol-6	0.84	-0.134	0.032	-0.225	0.044	Ol-7	0.43	-0.319	0.032	-0.507	0.044
Ol-7	0.60	-0.079	0.032	-0.139	0.044	Ol-8	2.72	-0.164	0.032	-0.294	0.054
Ol-8	0.96	-0.056	0.044	-0.108	0.068	Ol-9	9.40	-0.323	0.029	-0.502	0.050
Ol-9	0.34	+0.085	0.044	+0.104	0.068	Ol-10	1.19	-0.268	0.029	-0.411	0.050
Ol-10	0.49	+0.038	0.044	+0.066	0.068	Ol-11	7.08	-0.271	0.029	-0.413	0.050
Ol-11	1.24	-0.683	0.044	-1.023	0.068	Ol-12	1.36	-0.293	0.029	-0.439	0.050
Ol-12	0.72	-1.103	0.033	-1.680	0.067	Ol-13	1.44	-0.180	0.029	-0.258	0.050
Ol-13	0.42	+0.035	0.033	+0.039	0.067	Ol-14	0.31	-0.210	0.029	-0.321	0.050
Ol-14	0.26	+0.032	0.033	+0.029	0.067	Ol-15	0.72	-0.306	0.029	-0.480	0.050
Ol-15	0.48	-0.419	0.033	-0.620	0.067	Ol-16	0.40	-0.321	0.025	-0.454	0.051
Ol-16	0.46	+0.067	0.033	+0.083	0.067	Ol-17	0.49	-0.316	0.025	-0.473	0.051
Ol-17	0.53	+0.041	0.033	+0.045	0.067	Ol-18	1.28	-0.164	0.025	-0.278	0.051
Ol-18	0.67	-0.154	0.033	-0.236	0.067	Ol-19	0.51	-0.226	0.025	-0.368	0.051
Ol-19	0.41	-0.420	0.034	-0.629	0.060	Ol-20	0.62	-0.205	0.025	-0.316	0.051
Ol-20	1.02	-0.085	0.034	-0.149	0.060	Ol-21	0.47	-0.240	0.025	-0.374	0.051
Ol-21	1.42	+0.022	0.034	+0.014	0.060	Ol-22	1.02	-0.238	0.025	-0.401	0.051
Average		-0.206	0.155	-0.320	0.230	Average		-0.241	0.040	-0.388	0.074

95 % c.i. stands for 95 % confidence interval of the mean (for 9 replicate analyses of the same solution) and it integrates the long-term reproducibility based on replicate analyses of BHVO-1 standard (*S12*).

Table S3 Major element compositions of olivines from Kilauea Iki lava lake

Sample		SiO_2 (wt.%)	FeO (wt.%)	MgO (wt.%)	Fo (mole%)	T (^oC)
KI67-3-83.8	Max	35.5	31.4	32.6	64.9	1076
	Min	35.1	35.0	29.3	59.9	
KI75-1-139.3	Max	37.7	22.1	39.8	76.3	1084
	Min	36.8	29.3	33.6	67.1	
KI75-1-143.8	Max	38.2	21.0	41.2	77.8	1114
	Min	37.6	24.2	38.9	74.1	
KI79-3-166.1*	Max	38.9	17.9	43.0	81.0	1070
	Min	38.2	21.5	40.0	76.9	
KI79-3-172.9	Max	38.8	18.9	41.7	79.7	1108
	Min	37.2	23.7	38.6	74.4	
KI79-3-172.9*	Max	39.5	12.7	45.7	86.5	1110
	Min	38.9	18.2	41.6	80.3	
KI81-1-186.7	Max	38.0	22.7	38.7	75.3	1085
	Min	38.0	23.2	38.4	74.7	
KI81-1-205.4	Max	39.2	18.5	42.1	80.2	1135
	Min	37.8	19.0	42.0	79.7	
KI81-1-209.8*	Max	38.9	17.0	42.7	81.7	1135
	Min	38.8	17.8	41.9	80.7	
KI81-1-219.8	Max	38.3	19.0	42.2	79.9	1140
	Min	37.6	18.8	42.0	79.9	
KI81-1-306.7	Max	37.4	21.9	40.0	76.5	1087
	Min	36.9	24.0	38.5	74.1	
IKI-58	Max	40.0	13.0	46.6	86.5	1144
	Min	38.8	16.5	43.9	82.6	
IKI-22	Max	39.9	12.1	47.8	87.6	1216
	Min	39.4	14.2	45.9	85.2	

Major element compositions are analyzed by electronic microprobe from Helz (unpublished data). * Data are taken from Scowen et al. (*S16*). Fo is the mole fraction of forsterite in olivine (forsterite + fayalite). Quench temperatures are estimated by the MgO geothermometry (*S6*).

Table S4 Iron isotopic compositions of basalts, geostandards and meteorites analyzed during this study

Sample	Description	δ^{56}Fe	95 % c.i.	δ^{57}Fe	95 % c.i.
BHVO-1	Basalt (Kilauea, Hawaii)	+0.111	0.022	+0.156	0.033
Replicate		+0.100	0.033	+0.140	0.055
Average		+0.109	0.021	+0.154	0.033
T4D2#1	Basalt (Loihi, Hawaii)	+0.047	0.030	+0.073	0.050
T4D3#3	Basalt (Loihi, Hawaii)	+0.067	0.030	+0.099	0.050
T4D3#7	Basalt (Loihi, Hawaii)	+0.056	0.030	+0.118	0.050
BCR-1	Basalt (Columbia River, Oregon)	+0.088	0.028	+0.111	0.045
VS-90-56	Basalt (American-Antarctic ridge)	+0.179	0.028	+0.255	0.045
DTS-2	Dunite (Twin Sisters Mountain, WA)	-0.006	0.022	-0.004	0.040
AC-E	Granite (Ailsa Craig island, Scotland)	+0.330	0.032	+0.497	0.044
IF-G	BIF (Isua, Greenland)	+0.633	0.030	+0.945	0.050
Allende	Chondrite (CV3)	-0.010	0.030	-0.010	0.050

Replicate: repeat column chemistry from the same stock sample solution and analyzed by sample-standard bracketing method; 95 % c.i. stands for 95 % confidence interval of the mean (for 9 replicate analyses of the same solution) and it integrates the long-term reproducibility based on replicate analyses of BHVO-1 standard (*S12*).

References

S1. D. H. Richter, J. P. Eaton, K. J. Murata, W. U. Ault, H. L. Krivoy, *Chronological narrative of the 1959-60 eruption of Kilauea volcano, Hawaii*, U.S. Geol. Surv. Prof. Paper 537-E (1970), pp. 73.

S2. T. L. Wright, *Geological Society of America Bulletin* 84, 849 (1973).

S3. R. T. Helz, H. Kirschenbaum, J. W. Marinenko, *Geological Society of America Bulletin* 101, 578 (1989).

S4. R. T. Helz, in *Magmatic Processes: Physiochemical Principles* B. O. Mysen, Ed. (Geochem. Soc. Spec. Publ. 1, 1987) pp. 241-258.

S5. D. H. Richter, J. G. Moore, *U.S.G.S. Prof. Paper*, 537 (1966).

S6. R. T. Helz, C. R. Thornber, *Bulletin of Volcanology* 49, 651 (1987).

S7. R. T. Helz, *U.S.G.S. Prof. Paper* 1350, 691 (1987).

S8. R. T. Helz, H. Kirschenbaum, J. W. Marinenko, R. Qian, *U.S.G.S. Open File Report*, 94 (1994).

S9. F.-Z. Teng, M. Wadhwa, R. T. Helz, *Earth and Planetary Science Letters* 261, 84 (2007).

S10. P. B. Tomascak, F. Tera, R. T. Helz, R. J. Walker, *Geochimica et Cosmochimica Acta* 63, 907 (1999).

S11. N. Dauphas *et al.*, *Analytical Chemistry* 76, 5855 (2004).
S12. N. Dauphas, A. Pourmand, F.-Z. Teng, *Chemical Geology*, In review (2008).
S13. H. Taura, H. Yurimoto, K. Kurita, S. Sueno, *Physics and Chemistry of Minerals* 25, 469 (1998).
S14. H. Kirschenbaum, *U.S.G.S. Bull.* 1547, 55p. (1983).
S15. F. Albarede, B. L. Beard, in *Geochemistry of Non-Traditional Stable Isotopes* C. M. Johnson, B. L. Beard, F. Albarede, Eds. (Miner. Soc. of America, 2004), vol. 55, pp. 113-152.
S16. P. A. H. Scowen, P. L. Roeder, R. T. Helz, *Contributions to Mineralogy and Petrology* 107, 8 (1991).